Computational Mechanics 20 (1997) 170–175 © Springer-Verlag 1997

An element-free Galerkin method for three-dimensional fracture mechanics

N. Sukumar, B. Moran, T. Black, T. Belytschko

Abstract The application of a coupled finite element–element-free Galerkin (EFG) method to problems in three-dimensional fracture is presented. The EFG method is based on moving least square (MLS) approximations and uses only a set of nodal points and a CAD-like description of the body to formulate the discrete model. The EFG method is coupled with the finite element method which allows for the use of the EFG method in the crack region and the finite element method to model the remainder of the problem. Domain integral methods are used to evaluate stress intensity factors along the 3D crack front. Both planar and volume representations of the domain integrals are considered. The former require derivatives of stress and strain which are readily obtainable in the EFG method due to the C^1 continuity of the MLS approximations used here. Applications of the method to the determination of stress intensity factors along planar cracks in 3D are presented.

1 Introduction

The modeling of fracture and failure remains one of the most challenging problems in mechanics. Failure modeling is an essential ingredient in the lifetime prediction of critical components in structures such as aircraft, automobiles and pressure vessels. It also plays an important role in the development of advanced materials such as composites and in understanding their durability and integrity.

Finite element methods based on singular elements (Henshell and Shaw 1975; Barsoum 1977) as well as enriched elements (Benzley 1974; Gifford and Hilton 1978) are reasonably effective in the analysis of stationary cracks. However, the modeling of growing cracks (Gray et al. (1994)) presents automatic mesh generation difficulties and, in certain cases, manual intervention is required. No general purpose computational method currently exists which can handle crack growth in complex 3D bodies for arbitrary constitutive response without recourse to extensive remeshing.

In this paper, a coupled finite element–element-free Galerkin (EFG) method for problems in 3D fracture is presented. EFG methods (Belytschko et al. 1994; Lu et al. 1994) require only nodal data – no element structure is needed for the construction of the approximation. The approximating functions in EFG are moving least square approximants (MLS). They are not interpolants because the approximation does not pass through the data; this is often referred to as failure to satisfy the Kronecker delta property. As a consequence, essential boundary conditions cannot be specified directly. Typically, Lagrange multiplier methods or modified variational forms are used to implement the essential boundary conditions in the EFG method (Belytschko et al. 1994; Lu et al. 1994). A coupled finite element–element-free Galerkin method has been developed by Belytschko, Organ, and Krongauz (1995) and applied to fracture problems in two dimensions. This allows for the use of the EFG method in the crack region and the finite element method to handle complex geometries and essential boundary conditions.

In the following section, the governing equations for elastostatics are given. In Sect. 3, the element free Galerkin method together with its coupling to the finite element method is described. The enriched basis method for enhancement of the crack tip field is presented and the visibility and diffraction methods for construction of shape functions in the presence of the crack discontinuity are extended to three dimensions. In Sect. 4, domain integral methods for evaluation of stress intensity factors along a 3D crack front are described. Results for several benchmark problems in 3D fracture mechanics are presented in Sect. 5 and compared with solutions from the literature. Some final remarks are given in Sect. 6.

2 Element-free Galerkin method

2.1 Governing equations and weak form

We consider small displacement elastostatics, which is governed by the equation of equilibrium:

$$\nabla \cdot \boldsymbol{\sigma} + \mathbf{b} = 0 \text{ in } \Omega \tag{2.1}$$

where

$$\boldsymbol{\sigma} = \mathbf{C} : \boldsymbol{\epsilon}, \quad \boldsymbol{\epsilon} = \nabla_s \mathbf{u} \ . \tag{2.2}$$

Communicated by P. E. O'Donoghue, M. D. Gilchrist, K. B. Broberg, 6 January 1997

N. Sukumar, B. Moran, T. Black, T. Belytschko
Department of Civil Engineering, Northwestern University, Evanston, IL 60208, USA

Correspondence to: N. Sukumar

The authors are grateful for the research support of the Federal Aviation Administration, the Air Force Office of Scientific Research, and the National Science Foundation.

In the above equations, $\Omega \subset \mathbb{R}^3$ is the domain of the body, $\boldsymbol{\sigma}$ is the Cauchy stress tensor, $\boldsymbol{\epsilon}$ is the small strain tensor, $\mathbf{b}$ is the body force per unit volume, $\mathbf{C}$ is the material moduli tensor, $\mathbf{u}$ is the displacement, ∇ is the gradient operator, and ∇_s is the symmetric gradient operator.

The essential and natural boundary conditions are

$$\mathbf{u} = \bar{\mathbf{u}} \text{ on } \Gamma_u, \ \mathbf{n} \cdot \boldsymbol{\sigma} = \bar{\mathbf{t}} \text{ on } \Gamma_{\bar{t}} \ , \tag{2.3}$$

where Γ is the boundary of Ω, and $\bar{\mathbf{u}}$ and $\bar{\mathbf{t}}$ are prescribed displacements and tractions, respectively.

The weak form (principle of virtual work) is

$$\int_\Omega \nabla_s \delta\mathbf{v} : \boldsymbol{\sigma} \, d\Omega = \int_\Omega \delta\mathbf{v} \cdot \mathbf{b} \, d\Omega + \int_{\Gamma_t} \delta\mathbf{v} \cdot \bar{\mathbf{t}} \, d\Gamma \ \forall \ \delta\mathbf{v} \in \mathbb{H}^1_{\mathrm{E}}(\Omega) \tag{2.4}$$

2.2 Moving least square approximations

In the Element-Free Galerkin (EFG) method, the trial and test functions for the variational principle are constructed by moving least square (MLS) approximations (Lancaster and Salkauskas 1981). In the moving least square approximation, we let (Belytschko et al. 1994)

$$u^h(\mathbf{x}) = \sum_j^m p_j(\mathbf{x}) a_j(\mathbf{x}) \equiv \mathbf{p}^T(\mathbf{x}) \mathbf{a}(\mathbf{x}) \ , \tag{2.5}$$

where m is the number of terms in the basis, $p_j(\mathbf{x})$ are basis functions and $a_j(\mathbf{x})$ are the associated coefficients. For example, a linear basis in $3D$ is given by $\mathbf{p}^T(\mathbf{x}) = [1, \ x, \ y, \ z]$. The parameters $a_j(\mathbf{x})$ are found by minimizing the quadratic functional $J(\mathbf{x})$ given by

$$J(\mathbf{x}) = \sum_I^n w_I(\mathbf{x}) [\mathbf{p}^T(\mathbf{x}_I) \mathbf{a}(\mathbf{x}) - u_I]^2 \ , \tag{2.6}$$

where $w_I(\mathbf{x}) = w(\mathbf{x} - \mathbf{x}_I)$ is a non-negative weight function with compact support. On taking the extremum of $J(\mathbf{x})$ and substituting for $a_j(\mathbf{x})$ in Eq. (2.5), we obtain

$$u^h(\mathbf{x}) = \sum_I^n \sum_j^m p_j(\mathbf{x}) [\mathbf{A}^{-1}(\mathbf{x}) \mathbf{B}(\mathbf{x})]_{jI} u_I \equiv \sum_I^n \phi_I(\mathbf{x}) u_I \ , \tag{2.7}$$

where the EFG shape functions are given by

$$\phi_I(\mathbf{x}) = \sum_j^m p_j(\mathbf{x}) [\mathbf{A}^{-1}(\mathbf{x}) \mathbf{B}(\mathbf{x})]_{jI} \tag{2.8}$$

and u_I are nodal parameters; it is stressed that unlike the finite element method, u_I are not nodal values of $u^h(\mathbf{x}_I)$ because $u^h(\mathbf{x})$ is an approximant, and not an interpolant. In the above equation, the matrices $\mathbf{A}$ (moment matrix) and $\mathbf{B}$ are given by

$$\begin{aligned} \mathbf{A}(\mathbf{x}) &= \sum_I^n w_I(\mathbf{x}) \mathbf{p}(\mathbf{x}_I) \mathbf{p}^T(\mathbf{x}_I) \ , \\ \mathbf{B}(\mathbf{x}) &= [w_1(\mathbf{x}) \mathbf{p}(\mathbf{x}_1), \ldots, w_n(\mathbf{x}) \mathbf{p}(\mathbf{x}_n)] \ . \end{aligned} \tag{2.9}$$

The continuity of the shape function $\phi_I(\mathbf{x})$ depends on the continuity of the weight function $w_I(\mathbf{x})$ and that of the basis functions $\mathbf{p}(\mathbf{x})$. If $w_I(\mathbf{x}) \in C^k$ then it follows that $\phi_I(\mathbf{x}) \in C^k$ for a polynomial basis (Lancaster and Salkauskas, 1981).

In the EFG method, each node is associated with a domain of influence, often called a ball or support of the weight function $w_I(\mathbf{x})$, with $w_I(\mathbf{x}) > 0$ in the domain of influence and $w_I(\mathbf{x}) = 0$ outside it. Typically, domains of influence are spheres or parallelepiped domains. An example of a weight function for each of these domains can be derived from the quartic polynomial function:

$$f(r) = \begin{cases} 1 - 6r^2 + 8r^3 - 3r^4, & 0 \le r \le 1 \\ 0, & r > 1 \end{cases} \tag{2.10}$$

For a spherical domain of influence, the weight function is given by

$$w_I(\mathbf{x}) = f\left(\frac{d_I(\mathbf{x})}{d_{mI}}\right), \tag{2.11}$$

where $d_I(\mathbf{x}) = \|\mathbf{x} - \mathbf{x}_I\|_2$ and d_{mI} is a support parameter. The weight function for a parallelepiped domain of influence is given by

$$w_I(\mathbf{x}) = f\left(\frac{|x - x_I|}{d_{mIx}}\right) f\left(\frac{|y - y_I|}{d_{mIy}}\right) f\left(\frac{|z - z_I|}{d_{mIz}}\right), \tag{2.12}$$

where $w_I(\mathbf{x})$ has rectangular support with dimensions d_{mIx}, d_{mIy}, and d_{mIz} in the coordinate directions.

2.3 Enriched basis

To improve the representation of crack tip fields, especially for coarse nodal discretizations, Fleming et al. (1996) developed augmented trial function and enriched basis methods for fracture problems using the EFG method. The enriched basis approach is used in the present paper. As a 3D crack-front is approached, the asymptotic three-dimensional fields are plane strain in nature. The basis $\mathbf{p}(\mathbf{x})$ is therefore enriched by functions which incorporate the radial and angular behavior of the 2D plane strain near-tip displacement field (Fig. 1).

$$\begin{aligned} \mathbf{p}^T(\mathbf{x}) = \Bigg[& 1, \ x, \ y, \ z, \ \sqrt{r} \cos\frac{\theta}{2}, \sqrt{r} \sin\frac{\theta}{2}, \\ & \sqrt{r} \sin\theta \sin\frac{\theta}{2}, \ \sqrt{r} \sin\theta \cos\frac{\theta}{2} \Bigg] \ , \end{aligned} \tag{2.13}$$

where r and θ are polar coordinates in the $x_1 - x_2$ plane. For the enriched basis, if the weight function $w_I(\mathbf{x}) \in C^k$, then the shape function $\phi_I(\mathbf{x}) \in C^k$ in $\hat{\Omega} = \Omega - \Gamma_f$, where Γ_f is the crack front.

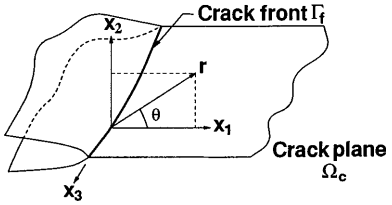

Fig. 1. Coordinate configuration for enriched basis function

2.4
Discontinuous and smooth approximations

The visibility criterion (Krysl and Belytschko 1996) defines a point $\mathbf{x}$ as being in the domain of influence of a node $\mathbf{x}_I$ if the line from $\mathbf{x}$ to $\mathbf{x}_I$ does not intersect the crack surface, i.e. if the point $\mathbf{x}$ is visible to an observer at the node when the crack is considered opaque (Fig. 2a). This criterion truncates nodal domains of influence along surfaces emanating from the crack front. This results in discontinuous weight functions and hence discontinuous shape functions along planes passing through the crack front. Krysl and Belytschko (1996) have presented a proof that the discontinuous approximation functions generated by the visibility criterion converge at the same rate as continuous EFG approximations; however, this does not rule out difficulties at points where the discontinuities pass through a singularity. Therefore, smooth approximations are used here.

In order to obtain smooth approximations with continuous shape functions, a technique called the diffraction method is used. The diffraction method in three dimensions is similar to its two-dimensional implementation described in (Organ et al. 1996). In the diffraction method, the weight function parameter $d_I(\mathbf{x})$ is modified so that, both the continuity of the weight function as well as the presence of the crack discontinuity in the model are preserved. The implementation for cracks in 3D is as follow (Krysl 1996):

1. Find $\mathbf{x}_p$, the intersection of the line from $\mathbf{x}$ to $\mathbf{x}_I$ with the crack surface.
2. Choose vector $\mathbf{b}_I$ in the direction from $\mathbf{x}_p$ to the closest point on Γ_f.
3. The vectors $\mathbf{b}_I$ and $\mathbf{x} - \mathbf{x}_I$ define a plane containing $\mathbf{x}_p$. The wrap-around point $\mathbf{x}_w$ is a point on the crack front in this plane which is closest to $\mathbf{x}_p$. The determination of $\mathbf{x}_w$ for a straight crack front is illustrated in Fig. 2b.
4. Let

$$s_0(\mathbf{x}) = \|\mathbf{x} - \mathbf{x}_I\|_2, \;\; s_1(\mathbf{x}) = \|\mathbf{x}_\mathbf{w} - \mathbf{x}_\mathbf{I}\|_2, \;\; \mathbf{s_2}(\mathbf{x}) = \|\mathbf{x} - \mathbf{x}_\mathbf{w}\|_2 \; . \tag{2.14}$$

The parameter $d_I(\mathbf{x})$ in the weight function is computed by

$$d_I(\mathbf{x}) = \left(\frac{s_1(\mathbf{x}) + s_2(\mathbf{x})}{s_0(\mathbf{x})} \right)^{\lambda} s_0(\mathbf{x}) \; , \tag{2.15}$$

where the exponent λ controls the size of the support behind the crack front. Suitable choices for λ are 1 or 2.

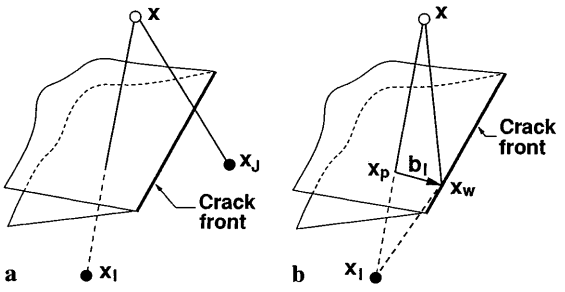

Fig. 2a,b. Shape function computations. **a** Visibility criterion and **b** Diffraction method

3
Coupled FE-EFG

The coupling of finite elements of EFG nodal data in a two-dimensional setting was proposed by Belytschko et al. (1995). The above approach is extended to three dimensions in this paper. We refer to Fig. 3 in order to illustrate the FE-EFG coupling in 3D. In order to preserve displacement continuity across the interface region Ω_I, the displacement $u_i^h(\mathbf{x})$ in the interface region is chosen as a weighted sum of the FE and EFG approximations. The displacement approximation in the entire domain Ω can be written as

$$u_i^h(\mathbf{x}) = \begin{cases} u_i^{\mathrm{EFG}}(\mathbf{x}) & \text{if } \mathbf{x} \in \Omega_E \\ \{1 - R(\mathbf{x})\} u_i^{\mathrm{FE}}(\mathbf{x}) + R(\mathbf{x}) u_i^{\mathrm{EFG}}(\mathbf{x}) & \text{if } \mathbf{x} \in \Omega_I \\ u_i^{\mathrm{FE}}(\mathbf{x}) & \text{if } \mathbf{x} \in \Omega_F \end{cases} \tag{3.1}$$

and therefore the nodal shape function $\tilde{\mathbf{\Phi}}_I(\mathbf{x})$ can be expressed as

$$\tilde{\mathbf{\Phi}}_I(\mathbf{x}) = \begin{cases} \phi_I(\mathbf{x}) & \text{if } \mathbf{x} \in \Omega_E \\ \{1 - R(\mathbf{x})\} N_I(\mathbf{x}) + R(\mathbf{x}) \phi_I(\mathbf{x}) & \text{if } \mathbf{x} \in \Omega_I \\ N_I(\mathbf{x}) & \text{if } \mathbf{x} \in \Omega_F \end{cases} \tag{3.2}$$

where $N_I(\mathbf{x})$ are the finite element shape functions, $\phi_I(\mathbf{x})$ are the EFG shape functions, and $R(\mathbf{x})$, which is a blending function, is defined as the sum of the FE shape functions associated with the interface EFG nodes:

$$R(\mathbf{x}) = \sum_{\substack{J \\ \mathbf{x}_J \in \Gamma_E}} N_J(\mathbf{x}) \; . \tag{3.3}$$

On substituting the trial and test functions in Eq. (2.4) and using the arbitrariness of nodal variations, the following discrete system of equations is obtained:

$$\boldsymbol{K}\mathbf{d} = \mathbf{f}^{\mathrm{ext}}, \tag{3.4}$$

where

$$\mathbf{K}_{IJ} = \int_\Omega \mathbf{B}_I^T \mathbf{D} \mathbf{B}_J \, \mathrm{d}\Omega, \quad \mathbf{f}_I^{\mathrm{ext}} = \int_{\Gamma_t} \tilde{\mathbf{\Phi}}_I^T \, \bar{t} d\Gamma + \int_\Gamma \tilde{\mathbf{\Phi}}_I^T \mathbf{b} \, \mathrm{d}\Omega \; . \tag{3.5}$$

In the above equation, $\tilde{\mathbf{\Phi}}_I$ is the shape function vector and $\mathbf{B}_I$ is the matrix of shape function derivatives. Further details on the FE-EFG coupling can be found in Belytschko et al. (1995) for the two-dimensional problem; the extension to the 3D case is straight-forward.

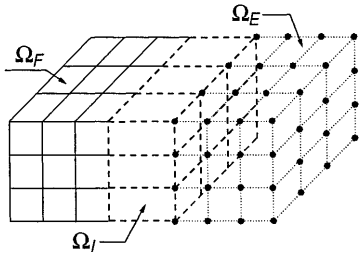

Fig. 3. FE-EFG coupling in three dimensions

4
Evaluation of stress intensity factors

Domain integral methods (Moran and Shih 1987; Nikishkov and Atluri 1987) are used to evaluate stress intensity factors along the 3D crack front. For the Mode-I crack problems considered here, the stress intensity factor at a point s on the crack front is given by

$$K_I(s) = \sqrt{\frac{J(s)E}{1-\nu^2}}\,. \tag{4.1}$$

With the normal to the crack front (and in the crack plane) oriented along the x_1-axis of a local coordinate system, the pointwise J-integral is given by

$$J(s) = \lim_{\Gamma\to 0}\int_{\Gamma(s)} H_{1\beta}n_\beta\,\mathrm{d}\Gamma,\ (\beta = 1,2) \tag{4.2}$$

where $H_{1j} = W\delta_{1j} - \sigma_{ij}u_{i,1}(i, j = 1,\ 2,\ 3)$. The volume form of the domain integral is given by (Moran and Shih 1987)

$$J(s) = -\frac{\int_V (H_{kj}q_{k,j} + H_{kj,j}q_k)\mathrm{d}V}{\int_{L_c} l_k v_k\,\mathrm{d}s}\ , \tag{4.3}$$

where V is a volume enclosing the crack front; $v_k(s)$ are components of the in-plane unit outward normal at s; $l_k(s)$ are components of an arbitrary unit vector at s lying in the plane of the crack; L_c is the perturbed segment along the crack front; and q_k is a C^0 vector field that is l_k on S_t, zero on S_0, and is arbitrary otherwise (Fig. 4a).

Alternatively, a planar domain integral representation of the crack-tip contour integral can be written as

$$J(s) = -\int_{A(s)} (H_{1\beta,\beta}q + H_{1\beta}q_{,\beta})\,\mathrm{d}A\ , \tag{4.4}$$

where $\beta = 1, 2$ and q is a test function which is unity on Γ, zero on C_0, and arbitrary otherwise (Fig. 4b).

In the absence of body force, inertia or material inhomogeneity, the energy-momentum tensor H_{kj} is divergence-free, i.e., $H_{kj,j} = 0$. Thus $H_{1\beta,\beta} + H_{13,3} = 0$ and hence the domain integral after some simplification can be written in the form

$$J(s) = -\int_{A(s)} (\sigma_{i3,3}u_{i,1} + \sigma_{i3}u_{i,13} + H_{1\beta}q_{,\beta})\,\mathrm{d}A. \tag{4.5}$$

It can be seen that this integral involves derivatives of stress and strain or second derivatives of displacement. In evaluating both the planar as well as volume integrals, the domains are confined to the EFG region of the model.

5
Results

Two problems are presented to evaluate the performance of the coupled FE-EFG method. A Galerkin procedure is used for the discretization, e.g. (Belytschko et al. 1994). In all problems, a background cell structure is used for Gaussian quadrature. In cells associated with EFG nodes, $6 \times 6 \times 6$ quadrature is used while in FE cells the quadrature is $2 \times 2 \times 2$. The elastic constants used in the computations are: Young's Modulus $E = 3 \times 10^7$ psi and Poisson's ratio $\nu = 1/3$. The enriched basis described in Sect. 2.3 and the smooth (diffraction method) weight function derived from the quartic polynomial function in Sect. 2.2 on spherical domains of influence are used in the numerical computations. An iterative solver (Balay et al. 1995) is used to solve the sparse system of linear equations.

5.1
Single edge-crack tension specimen

A single edge-crack tension specimen (Fig. 5a) with $h/b = 1.75$, $a/b = 1.0$, and $t/b = 3.0$ subjected to unit tractions in the z-direction is analyzed. The nodal discretization shown in Fig. 5b consists of 618 nodes, with the EFG nodes layered around the crack surface to capture the near-tip asymptotic solution. Stress intensity factors are computed along the crack front using volume and planar domain integrals.

In Fig. 6, the variation of the stress intensity factor (SIF) along the crack front is compared to the reference solution of Raju and Newman Jr. (1977). It is observed that the stress intensity factors are nearly uniform through most of the thickness with lower values near the free surface. The results obtained using this discretization are higher than that reported by Raju and Newman Jr. (1977) with less variation through the thickness. All the SIF results approach the plane strain value near the center of the specimen.

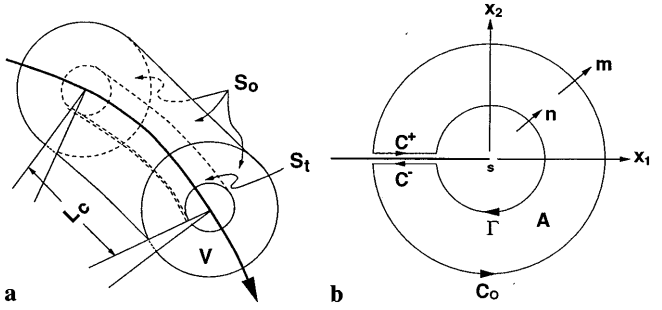

Fig. 4a,b. Domain integral representation for J-integral evaluation. **a** Volume form and **b** Planar form

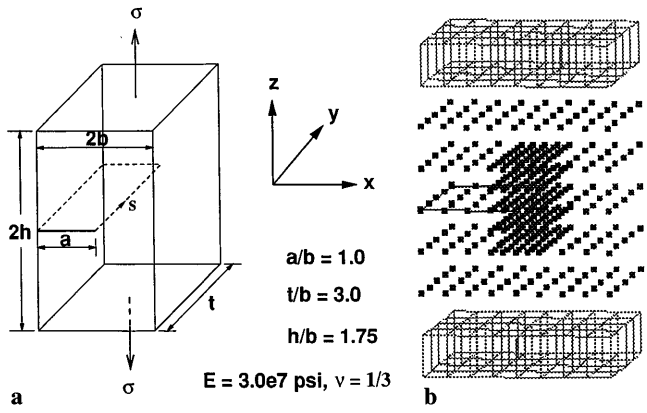

Fig. 5a,b. Single edge-crack specimen. **a** Geometry and **b** Nodal discretization

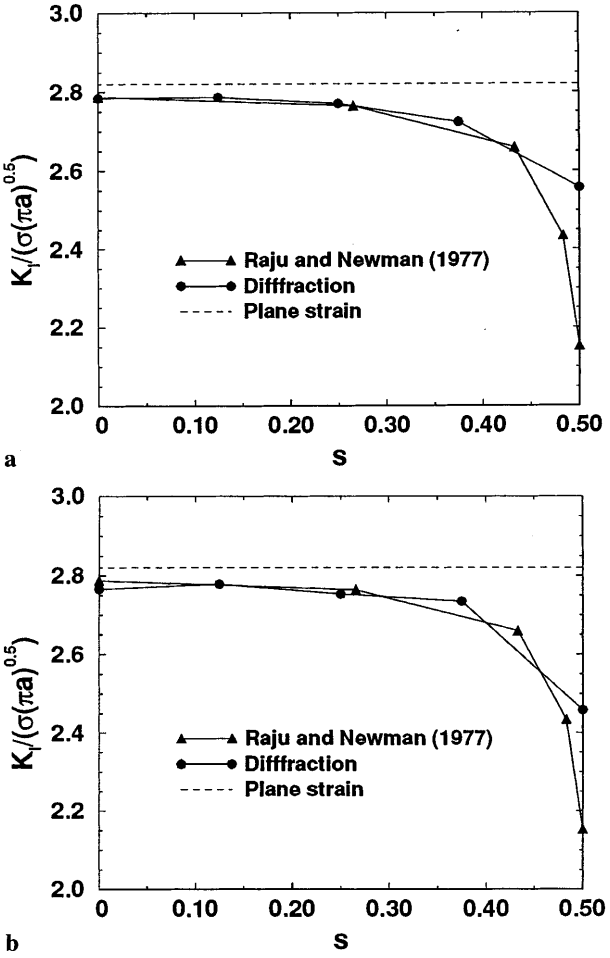

Fig. 6a,b. SIF computations for the edge-crack problem. **a** Volume domain integral and **b** Planar domain integral

5.2
Penny-shaped crack in an infinite body under tension

Consider a penny-shaped crack of radius a in a cylinder of radius R $(a/R = 0.2)$ under mode I loading conditions. The body is subjected to unit tractions in the z-direction. Since the specimen radius is significantly greater than the crack radius, the model is assumed to adequately represent the problem of a penny-shaped crack in an infinite body. The nodal discretization consists of 2642 nodes: 552 EFG nodes in the immediate vicinity of the crack front and 2090 FE nodes in regions away from the crack discontinuity. The stress intensity factors are calculated using the volume form of the domain integral at 11.25° intervals around the crack front. In Fig. 7, the SIF results obtained by the FE-EFG computations are compared to the exact solution. It is observed that the SIF results are in excellent agreement with the exact solution.

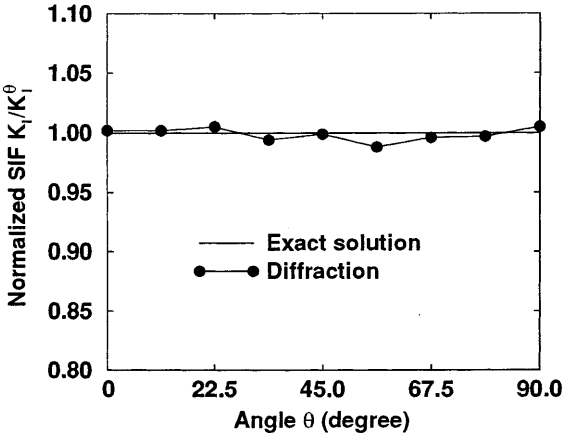

Fig. 7. SIF computations for the penny-shaped crack under tension $(K_I^e = 2\sigma\sqrt{a/\pi})$

6
Conclusions

In this paper, the capabilities of the FE-EFG method in three-dimensional fracture mechanics applications are explored. An enriched basis is used in which four linearly independent components of the two-dimensional plane strain near-tip asymptotic crack field are included. It is adapted to three dimensions by using its radial and angular dependence in a plane normal to the tangent vector at a point on the crack front. In order to assess the methods' accuracy, potential, and to establish parametric settings for EFG in solving crack problems, two well-known benchmark three-dimensional crack problems are considered. The stress intensity factors obtained in this study for both problems are found to be in good agreement with SIF values reported in the literature. This preliminary study has indicated that the Element-Free Galerkin method provides accurate stress intensity factors for planar 3D fracture problems. In future studies, the impetus will be towards applying the EFG method to modeling three-dimensional crack propagation phenomena with emphasis on both, planar, as well as non-planar crack surfaces with curved crack fronts.

References

Balay, S.; McInnes, L. C.; Gropp, W.; Smith, B. (1995): PETSc 2.0 users manual. Technical Report ANL 95/11, Argonne National Laboratory

Barsoum, R. S. (1977): Triangular quarter-point elements as elastic and perfectly-plastic crack tip elements. Int. J. Num. Meth. Eng. 11, 85–98

Belytschko, T.; Lu, Y. Y.; Gu, L. (1994): Element-free Galerkin methods. Int. J. Num. Meth. Eng. 37, 229–256

Belytschko, T.; Organ D.; Krongauz, Y. (1995): A coupled finite element–element-free Galerkin method. Comp. Mech. 17, 186–195

Benzley, S. E. (1974): Representation of singularities with isoparametric finite elements. Int. J. Num. Meth. Eng. 8, 537–545

Fleming, M.; Chu, Y. A.; Moran, B.; Belytschko, T. (1997): Enriched element-free Galerkin methods for crack tip fields. Int. J. Num. Meth. Eng. 40, 1483–1504

Gifford Jr., L. N.; Hilton, P. D. (1978): Stress intensity factors by enriched finite elements. Eng. Fract. Mech. 10, 485–496

Gray, L. J.; Potyondy, D. O.; Lutz, E. D.; Wawrzynek, P. A.; Martha, L. F.; Ingraffea, A. R. (1994): Crack propagation modeling. Math. Models Methods Appl. Sci. 4, 179–202

Henshell, R. D.; Shaw, K. G. (1975): Crack tip finite elements are unnecessary. Int. J. Num. Meth. Eng. 9, 495–507

Krysl, P. (1996): Private Communication

Krysl, P.; Belytschko, T. (1996): Element-free Galerkin method: Convergence of the continuous and discontinuous shape functions. Comput. Meth. Appl. Mech. Eng. (to appear)

Lancaster, P.; Salkauskas, K. (1981): Surfaces generated by moving least squares methods. Math. Comput. 37, 141–158

Lu, Y. Y.; Belytschko, T.; Gu, L. (1994): A new implementation of the element free Galerkin method. Comput. Meth. Appl. Mech. Eng. 113, 397–414

Moran, B.; Shih, C. F. (1987): Crack tip and associated domain integrals from momentum and energy balance. Eng. Fract. Mech. 27 (6), 615–641

Nikishkov, G. P.; Atluri, S. N. (1987): Calculation of fracture mechanics parameters for an arbitrary three-dimensional crack by the 'equivalent domain integral method'. Int. J. Num. Meth. Eng. 24, 1801–1821